

# UC San Diego

## UC San Diego Previously Published Works

### Title

Extreme-ultraviolet spectral purity and magnetic ion debris mitigation by use of low-density tin targets

### Permalink

<https://escholarship.org/uc/item/7w493333>

### Journal

Optics Letters, 31(10)

### Authors

Harilal, S S  
Tillack, Mark S  
O'Shay, Beau  
et al.

### Publication Date

2006

Peer reviewed

# **Extreme ultraviolet spectral purity and magnetic ion debris mitigation with low density tin targets**

**S. S. Harilal, M. S. Tillack, Y. Tao, B. O'Shay**

*Center for Energy Research, University of California San Diego, 9500 Gilman Drive,  
La Jolla, CA 92093-0438*

**R. Paguio and A. Nikroo**

*General Atomics, San Diego, CA 92186*

We investigate the extreme ultraviolet (EUV) emission from targets containing tin as an impurity and advantages of these targets for ion debris mitigation using a magnetic field. The EUV spectral features were characterized using a transmission grating spectrograph. The in-band EUV emission energy was measured using an absolutely calibrated calorimeter. The ion flux coming from the plume was measured using a Faraday cup. Our studies indicate that 0.5% Sn density is necessary to obtain a conversion efficiency very close to full density tin. The usage of tin doped low-Z targets provide narrower unresolved transition array and facilitate better control over energetic ions in the presence of a moderate magnetic field of 0.64 T.

Key words: EUV lithography source, debris mitigation, laser produced tin plasma, plasma diagnostics, EUV spectroscopy

Extreme ultraviolet lithography (EUVL) at 13.5 nm is a leading candidate for next generation high volume patterning<sup>1</sup>. The essential requirement for enabling this technology is to have a reliable, clean and powerful light source around 13.5 nm. The laser-produced tin plasma (LPP) has a strong potential to be the future EUV light source and offers higher conversion efficiency (CE) compared to xenon-based sources<sup>1-3</sup>. However, apart from high CE, debris from the source and hence optics lifetime and spectral purity are the main concerns being addressed by the light source developers. Condensable targets like tin can pose deleterious debris problems in commercial lithography processes. The biggest concern is the fast ions from the plasma that are expected to significantly damage the collector mirror by means of ion-induced mixing of multi-layer mirror (MLM), by etching and implantation of the MLM coating, which is located near the EUV light source<sup>4</sup>. Hence application of practical EUV sources without proper debris mitigation results in an EUVL tool with unacceptable operational lifetime. Consequently various concepts have been proposed for controlling the debris from plasma including tape targets<sup>5</sup>, ambient gas for moderating the species<sup>6</sup>, foil trap<sup>7</sup>, cavity confinement<sup>3</sup>, application of electrostatic repeller fields<sup>8,9</sup>, and magnetic fields<sup>10,11</sup>. The other concept for reducing the debris is the usage of mass limited targets, where the numbers of the tin atoms are just enough to provide bright unresolved transition array (UTA) emission<sup>9</sup>.

Opacity effects significantly influence the EUV spectral energy from laser-produced tin plasma. Fujikoa et. al.<sup>12,13</sup> studied opacity effects and suggested the optical thickness of the tin plasma should be controlled by changing the initial target density. One of the most effective ways in accomplishing this is to use Sn atoms as a measurable

impurity in the EUVL target. In this letter we report the advantages of using low-Z targets with tin as an impurity as well as effective mitigation of ion debris using a magnetic field. Our results show that the density of tin required for bright UTA is  $\sim 0.5\%$  and UTA from these targets provide high spectral purity in comparison with solid density tin. A moderate magnetic field of 0.64 T is found to be very effective for controlling energetic ions from tin doped low-Z targets. .

For producing plasma, 1064 nm, 10 ns (full width at half maximum, FWHM) pulses from an Nd: YAG laser was used. The target was mounted in a vacuum chamber with a base pressure  $\sim 10^{-6}$  Torr. The 60  $\mu\text{m}$  diameter focal spot was measured using an optical imaging technique and remained unchanged during the experiment. The EUV emission from the plasma was measured using a transmission grating spectrograph (TGS) equipped with a 10,000 lines/mm grating and a back illuminated x-ray CCD camera. An absolutely calibrated Jenoptik EUV calorimeter was used for measuring the CE of the in-band radiation at 13.5 nm with 2% bandwidth. The principle of operation of the EUV calorimeter was filtering out the in-band range from the broadband incidence spectrum of the EUV source by using a Zr filter and two Mo/Si multi-layer mirrors. A photodiode (IRD, SUXV-100) sensitive to EUV range was used for detection. The EUV calorimeter and TGS were placed  $45^\circ$  with respect to the laser beam. Since the EUV plasma emission has got an approximately hemispherical symmetry<sup>14</sup>, the output from the energy monitor was simply integrated over a  $2\pi$  solid angle for obtaining CE.

The ion emission from the plume was monitored using a Faraday cup. The ambient magnetic field is supplied by an assembly of 2 permanent magnets ( $B_{\text{max}} = 1.2$  T) mounted in a steel core, creating a uniform field configuration over a volume  $5 \text{ cm} \times 2.5$

cm  $\times$  1.5 cm. The maximum magnetic field is 0.64 T and is nearly uniform along the direction of plume expansion<sup>15</sup>.

For fabricating the tin doped foam bead targets, the required amount of tin oxide (SnO<sub>2</sub> contains 78.8% of Sn by mass) is dispersed in a resorcinol formaldehyde (RF, density 100mg/cc) solution and dried. The target beads are  $\sim$  500 microns in diameter, and the morphology of the target was verified using a scanning electron microscope. EUV spectral measurements with varying concentration of Sn showed the brightness of UTA was more or less constant when the tin density dropped from 100% to 0.5% indicating that plasma is optically thick to 13.5 nm. Typical UTA recorded from full density tin target and 0.5% Sn doped foam targets are given in fig. 1. The UTA emission is concentrated around 13.5 nm arising from  $4p^6 4d^n - 4p^5 4d^{n+1} + 4p^6 4d^{n-1} 4f$  transitions of various Sn ions ranging from Sn<sup>6+</sup> to Sn<sup>14+</sup> with occupancy in the range of  $n = 2$  to  $n = 8$  as shown by Cummins et. al.<sup>16</sup>. The spectral features of Sn doped foam targets also contained oxygen emission lines. They are identified as O<sup>5+</sup> lines at 12.99 nm (2p-4d) and 15.00 nm (2s-3p).

Compared to the solid Sn slab, the UTA emission from Sn doped foam targets showed reduced continuum emission and a narrowed spectrum peaked at 13.5 nm. Fujioka et. al.<sup>13</sup> also observed similar narrowing of the UTA using low density targets and attributed it to a reduction of satellite emission from multiply excited Sn ions, and less opacity broadening during the radiation transport. Tomie and co-workers<sup>17</sup> also reported narrower UTA profile from cavity confined Sn plasma. Theoretical calculations showed<sup>16,18</sup> that the core tin ions contributing to the UTA at 13.5 nm range from Sn<sup>10+</sup> - Sn<sup>13+</sup> while lower charged species (Sn<sup>6+</sup> - Sn<sup>9+</sup>) emit at the longer wavelength side of the

UTA (>14 nm). The UTA from the 0.5% Sn targets showed reduction of emission at wavelength > 14 nm in comparison with 100 % Sn. It indicates the decrease in Sn density leads to the quenching of lower ionization states.

Figure 2 shows the dependence of CE with laser intensity. All the measurements were done with a laser beam spot size of 60  $\mu\text{m}$ . The CE of full density tin is found to peak around  $4 \times 10^{11} \text{ W/cm}^2$  and obtained a maximum CE  $2.04 \pm 0.1 \%$  while the highest CE obtained for 0.5% density tin is  $1.95 \pm 0.1 \%$  peaked at  $8 \times 10^{11} \text{ W/cm}^2$ . It shows a small density of tin is necessary to obtain the CE very close to the full density tin. White et. al<sup>18</sup> reported that CE measurement is very sensitive to the Sn charge state distribution. According to Fig 2. a higher laser intensity is required to reach the same  $\langle Z \rangle$  in the low Sn density target than the full Sn density target. From figure 1. one can infer that for the same peak intensity, the measured CE for the 0.5% Sn density target has to be smaller than for the 100% Sn density target due to the steeper slope of the UTA feature on the low wavelength side.

Controlling and mitigating the fast ions from the tin target is one of the bigger challenges to overcome in order to successfully implement such EUVL sources as they are expected to significantly damage the collector mirror<sup>4</sup>. The ion debris measurements were carried out in the presence and absence of magnetic field using a Faraday cup placed at 15 cm from the target and at an angle approximately  $12^\circ$  with respect to the target normal. It should be noted that the distribution of ions in a laser created plasma are best approximated by single charge dependent  $\text{Cos}^n$  function where the value of n increases with charge state and decreases with atomic mass<sup>19</sup>. The location of the Faraday cup is based on the fact that in the EUVL tool, the collector mirror is expected to be

placed ~15 cm from the source. Figure 3 shows a comparison of Faraday cups signals between full-density tin and 0.5% Sn doped foam targets in the presence and absence of a transverse magnetic field of 0.64 T. For applying magnetic field, the target placed a distance of 1 cm from the pole edges resulting in a uniform magnetic field along the plume's expansion direction<sup>15</sup>.

The kinetic energy distribution of the tin ions showed energies up to 5 keV with a peak ion flux at 1.2 keV. In the presence of the magnetic field, the tin ions are found to have considerably slowed down, but are not fully mitigated. It is also worth to note that the collector charge yield considerably increased in the presence of B field may be caused by the deflection of ions by the field. The ions coming out from the foam targets have maximum probable velocity  $\sim 1 \times 10^7$  cm/s which is considerably larger than the expansion velocity of Sn ions from pure tin targets ( $\sim 4.3 \times 10^6$  cm/s). But the magnetic field showed more influence in controlling light ions and from figure 3 it can be seen that the ion flux is reduced by more than one order of magnitude for the foam target. Optical time of flight studies showed neutrals can also be effectively controlled by the magnetic field due to confinement of the plume<sup>10,15</sup>.

When a plume expands into a B field, the plume behavior is mainly controlled by thermal beta<sup>20</sup> ( $\beta_t = 2\mu_0nkT/B^2$ ) and directed beta ( $\beta_d = \mu_0nmv^2/B^2$ ) where n, T and v are the density, temperature and velocity respectively. Our analysis showed that thermal beta ( $\beta_t$ ) of the plasma approaches unity ~100 ns after formation of the plasma. After the initial conversion of thermal energy to directed energy, directed  $\beta$  ( $\beta_d$ ) becomes an important parameter. In the early phase of the plume expansion,  $\beta_d$  is on the order of a few thousand, indicating that the plume is in the regime of diamagnetic expansion.

Diamagnetic currents exclude the magnetic field from the interior of the plume, and may interact with the steady state magnetic field through the  $\mathbf{J} \times \mathbf{B}$  force, tending to inhibit plume expansion. The laser-produced plasma diamagnetic cavity (magnetic bubble) expands until the total excluded magnetic energy becomes comparable to the total plasma energy<sup>15</sup>. Visible spectroscopic studies<sup>21</sup> indicated that, at late stages the bulk ion component was  $\text{Sn}^+$ , whose Larmor radius is  $\sim 3.5$  cm and its value decreases with increasing charge state. The tin doped foam targets contain different elements with various atomic percentages (Sn (1.8%), O (17.2%), C (27%) and H (54%)) showing the main contribution is from low- $Z$  elements. Even though Faraday cup measurements showed nearly double the velocity for ions emanating from tin doped foam targets compared with solid Sn, the  $\beta_d$  is found to be much lower for tin doped foams because of the lower average mass.

In conclusion, we report the effectiveness of the tin doped foam target for ion mitigation using a transverse magnetic field. A moderate magnetic field of 0.64 T is found to be effective for mitigating energetic ions by more than one order when the tin is doped as an impurity in a low- $Z$  target while the field only slowed down tin ions coming out from the fully density tin plasma. The low-density tin targets also provided high spectral purity by narrower UTA spectrum. The CE measurements showed 0.5% Sn density is necessary to obtain a CE that obtained with full density Sn.



References:

1. B. Marx, Laser Focus World **39**, 34 (2003).
2. R. C. Spitzer, R. L. Kauffman, T. Orzechowski, D. W. Phillion, and C. Cerjan, J. Vac. Sci. Tech. **11**, 2986 (1993).
3. T. Tomie and T. Aota, Phy. Rev. Lett. **94**, 015004 (2005).
4. J. P. Allain, A. Hassanein, M. Nieto, V. Titov, P. Plotkin, E. Hinson, and C. Chrobak, Proc. of SPIE **5751**, 1110 (2005).
5. S. J. Haney, K. W. Berger, G. D. Kubiak, P. D. Rockett, and J. Hunter, Appl. Opt. **32**, 6934 (1993).
6. F. Flora, L. Mezi, C. E. Zheng, and F. Bonfigli, Europhys. Lett. **56**, 676 (2001).
7. J. Pankert, R. Apetz, K. Bergmann, A. List, M. Loeken, C. Metzmacher, W. Neff, and S. Probst, Proc. of SPIE **5751**, 260 (2005).
8. K. Takenoshita, C. S. Koay, and M. Richardson, Proc. of SPIE **5037**, 792 (2003).
9. M. Richardson, C. S. Koay, K. Takenoshita, C. Keyser, and M. Al-Rabban, J. Vac. Sci. Tech. **22**, 785 (2004).
10. S. S. Harilal, B. O'Shay, and M. S. Tillack, J. Appl. Phys. **98**, 036102 (2005).
11. G. Niimi, Y. Ueno, K. Nishigori, T. Aota, H. Yashiro, and T. Tomie, Proc. of SPIE **5037** (2003).
12. S. Fujioka, H. Nishimura, K. Nishihara, A. Sasaki, A. Sunahara, T. Okuno, N. Ueda, T. Ando, Y. Tao, Y. Shimada, K. Hashimoto, M. Yamaura, K. Shigemori,

- M. Nakai, K. Nagai, T. Norimatsu, T. Nishikawa, N. Miyanaga, Y. Izawa, and K. Mima, *Phy. Rev. Lett.* **95**, 235004 (2005).
13. S. Fujioka, H. Nishimura, T. Okuno, Y. Tao, N. Ueda, T. Ando, H. Kurayama, Y. Yasuda, S. Uchida, Y. Shimada, M. Yamaura, Q. Gu, K. Nagai, T. Norimatsu, H. Furukawa, A. Sunahara, Y. Kang, M. Murakami, K. Nishihara, N. Miyanaga, and Y. Izawa, *Proc. of SPIE* **5751**, 578 (2005).
  14. Y. Tao, F. Sohbatzadeh, H. Nishimura, R. Matsui, T. Hibino, T. Okuno, S. Fujioka, K. Nagai, T. Norimatsu, K. Nishihara, N. Miyanaga, Y. Izawa, A. Sunahara, and T. Kawamura, *Appl. Phys. Lett.* **85**, 1919 (2004).
  15. S. S. Harilal, M. S. Tillack, B. O'Shay, C. V. Bindhu, and F. Najmabadi, *Phy. Rev. E* **69**, 026413 (2004).
  16. A. Cummings, G. O'Sullivan, P. Dunne, E. Sokell, N. Murphy, and J. White, *J. Phys. D* **38**, 604 (2005).
  17. T. Aota, H. Yashiro, Y. Ueno, and T. Tomie, *Proc. of SPIE* **5037**, 742 (2002).
  18. J. White, P. Hayden, P. Dunne, A. Cummings, N. Murphy, P. Sheridan, and G. O'Sullivan, *J. Appl. Phys.* **98**, 113301 (2005).
  19. A. Thum-Jager and K. Rohr, *J. Phys. D* **32**, 2827 (1999).
  20. B. H. Ripin, E. A. McLean, C. K. Manka, C. Pawley, J. A. Stamper, T. A. Peyser, A. N. Mostovych, J. Grun, A. B. Hassam, and J. Huba, *Phy. Rev. Lett.* **59**, 2299 (1987).
  21. S. S. Harilal, B. O'Shay, M. S. Tillack, and M. V. Mathew, *J. Appl. Phys.* **98**, 013306 (2005).

### **Figure Captions:**

Fig. 1. The UTA obtained from full density tin and 0.5% Sn density. The UTA spectrum from tin doped foam targets showed distinct narrowing. Both the spectra were recorded with a laser intensity of  $4 \times 10^{11} \text{ Wcm}^{-2}$ .

Fig. 2. Estimated CE for full density Sn and 0.5% Sn doped foam target at various laser intensities.

Fig. 3. Typical ion TOF signals recorded for full density (a) and 0.5 % density (b) tin in the presence and absence of magnetic field. A magnified version of the TOF profile obtained from 0.5 % Sn in the presence of magnetic field is given in the inset of (b)

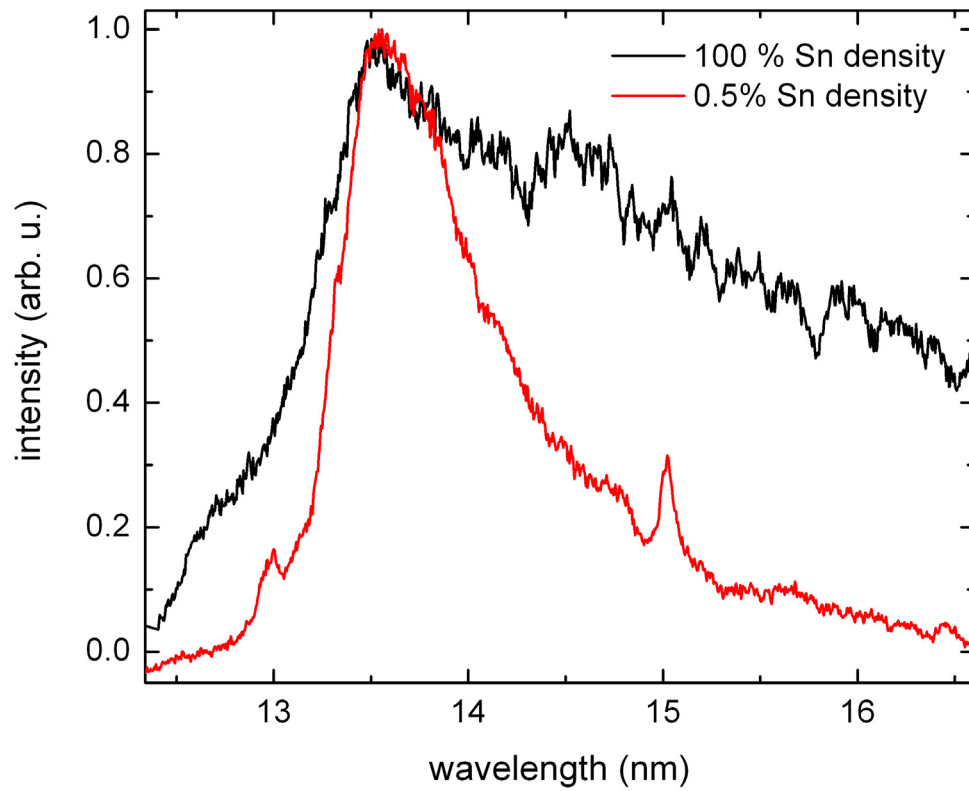


Fig.1

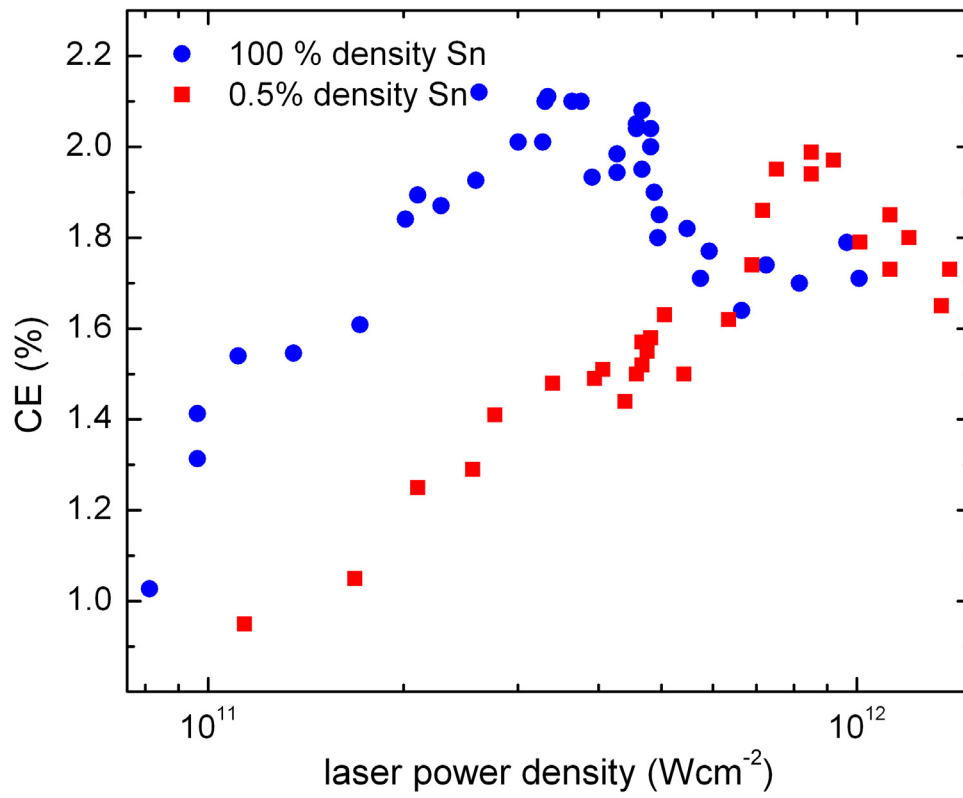


Fig. 2.

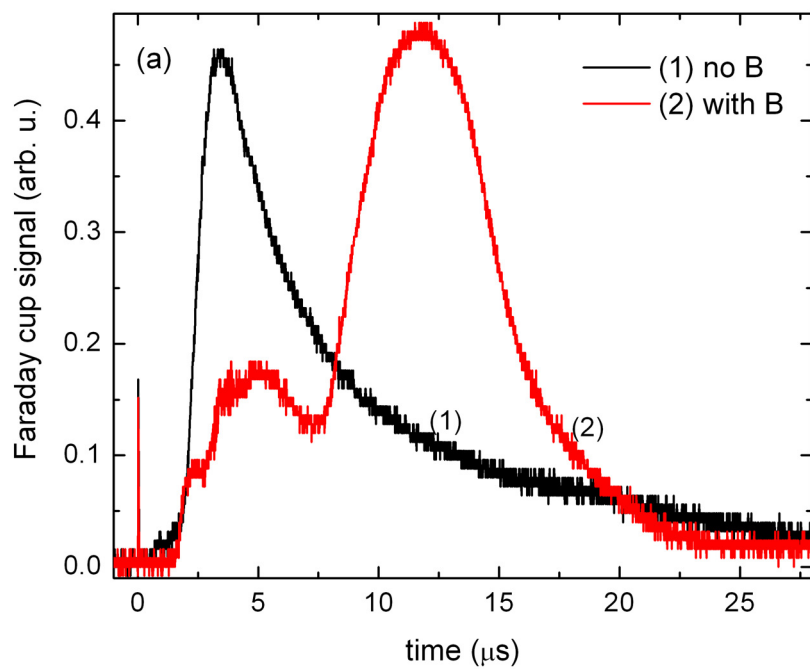


Fig.3(a)

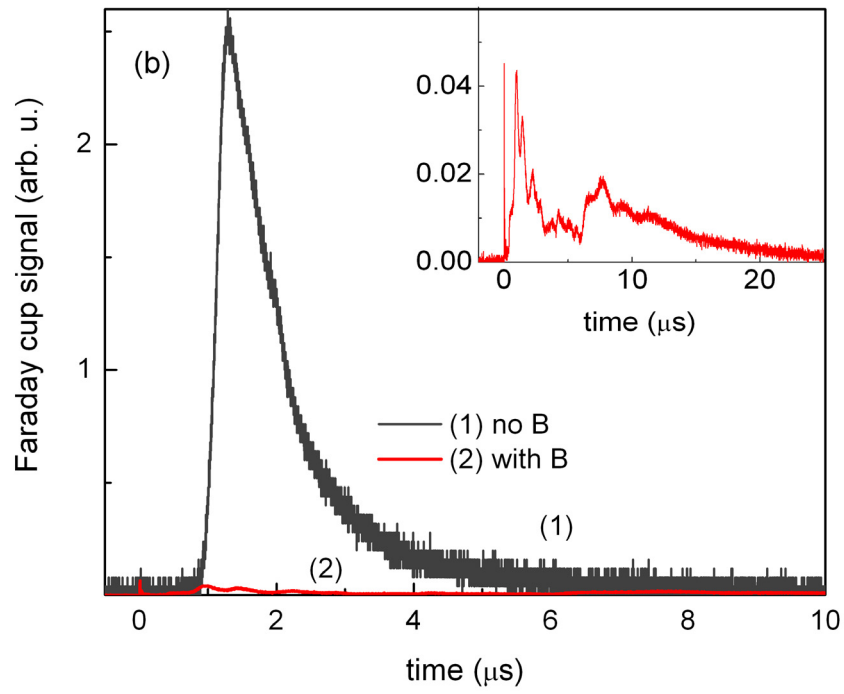


Figure 3 (b).